Surface relaxations in hydroxyapatite

2000 J. Phys.: Condens. Matter 12 9829

(http://iopscience.iop.org/0953-8984/12/48/302)

J. Phys.: Condens. Matter **12** (2000) 9829–9841. Printed in the UK PII: S0953-8984(00)16036-9

Surface relaxations in hydroxyapatite

W T Lee, M T Dove and E K H Salje

Department of Earth Sciences, University of Cambridge, Downing Street, Cambridge CB2 3EQ, UK

E-mail: wlee@esc.cam.ac.uk (W T Lee), martin@esc.cam.ac.uk (M T Dove) and es10002@esc.cam.ac.uk (E K H Salje)

Received 2 August 2000, in final form 12 October 2000

Abstract. Relaxation processes due to two opposite surfaces in a slab of hydroxyapatite with two (100) free surfaces are reported. Interatomic potentials for hydroxyapatite, chloroapatite and fluoroapatite were refined using elastic and vibrational data. Systems with two free (100) surfaces were relaxed. It was found that the relaxation processes which occurred at the surface included the polarization of layers close to the surface, distortion of the channels in which the hydroxide ions sit and distortion of the tetrahedral phosphate ions. Some of these relaxations only occur in the unit cells closest to the surface; others persist for a few unit cells distance into the bulk. The implications of these results for the growth morphology of hydroxyapatite in bones are discussed.

1. Introduction

In this work we report the results of an interatomic potential study of relaxation processes at the (100) surfaces of hydroxyapatite crystals. The motivation for this study is that such relaxation processes may be relevant to explaining the growth morphology of apatite in bones. The apatite in bones is a calcium-deficient, carbonated form of hydroxyapatite. The crystals in bone apatite are very small (length 50 nm, breadth 25 nm and thickness up to 4 nm) and have a platelet morphology (Weiner and Wagner 1998). Because the crystals are so small, their morphology should be consistent with the crystal symmetry, but this is not the case. Hydroxyapatite has hexagonal symmetry and the hexagonal *c*-axis of the crystals lies in the plane of the platelet. It has been shown theoretically that surface relaxations can have a symmetry-breaking effect on growth morphologies, producing equilibrium platelet morphologies even when these are inconsistent with the symmetry of the crystal (Lee *et al* 1999), although no examples of this occurring in nature have been confirmed so far. It may be that such an effect is responsible for the growth morphology of bone apatite.

The platelet growth mechanism referred to above is due to the overlap of relaxations from opposite surfaces. There is a free energy associated with these relaxations which is modified when they overlap. Mathematically, this overlap term in the free energy of the surface relaxations takes the form of a short-range interaction between surfaces. If this interaction is attractive and of comparable magnitude to the surface energy, then a platelet morphology will result. This study of surface relaxations is unusual therefore, in that we investigated relaxations in systems with two surfaces rather than a single surface. In order to investigate relaxations in such systems, the method of interatomic potentials was used. We derived potentials for the minerals hydroxyapatite, chloroapatite and fluoroapatite by fitting to empirical data. In this method, empirical data such as structures, elastic constants and phonon frequencies are used

0953-8984/00/489829+13$30.00

as input. Starting from an initial guess at an interatomic potential set, the calculated values of the empirical data are compared with their observed values. The parameters describing the potentials are then adjusted to maximize agreement between the calculated and observed values. In section 2 we describe in more detail the methods used to refine the interatomic potential model and compare the predictions of the model with experiment and with the fluoroapatite model developed by Meis *et al* (2000)

Having obtained an interatomic potential set, we calculated the structural relaxation of hydroxyapatite systems with two (100) surfaces. This was achieved using the program MARVIN (Gay and Rohl 1995). The relaxation processes investigated were: polarization of the atomic layers, distortion of the hydroxide channels and distortion of the phosphate ions. We found that the polarization relaxation extended several unit cells' distance into the bulk of the material. Such a relaxation generates an interaction energy between surfaces, which we evaluated by calculating the surface energy of the system as a function of the separation of the surfaces. This revealed a short-range interaction between the surfaces acting over a distance of several unit cells. These results are presented in section 3.

In the final section we consider the implications of our results for explaining the growth morphology of bone apatite. Although the results presented here do not constitute an explanation of the morphology on their own, we believe that they may form part of an explanation. The reason for this is that this study only considers pure hydroxyapatite in contact with vacuum. These are not the conditions under which bone apatite grows. Bone apatite is not pure hydroxyapatite but contains many impurity species of which the most important are carbonate impurities. In addition, the apatite surface will be in contact with water and biological macromolecules such as collagen. Both the surface relaxation and the surface energy of biological apatites may be modified by the growth conditions to such an extent that the platelet growth mechanism is activated. This is discussed in more detail in section 4.

Lastly, in an appendix, we consider the extent to which we expect an interatomic potential model, refined against bulk phonon frequencies and elastic constants, to be successful in predicting surface relaxations and surface interaction energies.

2. The interatomic potential model

To investigate the surface structure of hydroxyapatite we decided to use the method of empirical interatomic potentials. Although this is presumed to be less accurate than electronic structure calculations, it requires much less computing power and thus allows larger systems to be investigated. The potentials between atoms were chosen to maximize agreement between calculated properties and their experimental values. The following experimental properties were used as data to refine against.

(1) The structures of hydroxyapatite, chloroapatite and fluoroapatite. These were given by Hughes *et al* (1989).
(2) Elastic constants. The only measurements of elastic constants we could find were by Bhimasenachar (1945). This work gives the elastic constants for an unspecified form of apatite. Since materials with similar structures and compositions have similar elastic constants, we decided to refine the elastic constants of each form of apatite against these elastic constants.
(3) Vibrational modes of the phosphate ion. These were given by Farmer (1974).

The interatomic potentials were refined against these data using GULP (Gale 1997). The program GULP contains an option which allows the fitting of empirical data to an empirical

potential model. As a starting point a set of potentials obtained from the Royal Institution Database www.ri.ac.uk/Potentials/ were used (Sanders *et al* 1984, Bush *et al* 1994, Parker and Baram 1996). The potentials were: Coulomb potentials due to formal charges on ions, Buckingham potentials between atoms that were in contact (to prevent the structure collapsing), three-body potentials within the phosphate ion (the initial guess value was taken from a silicate three-body potential) and dispersive interactions between oxygen atoms. The relax fitting option was used, which relaxes the structure (subject to symmetry constraints) and then calculates a sum of squares S:

$$S = \sum_{\text{observables}} w(f_{calc} - f_{obs})^2 \tag{2.1}$$

where f_{calc} and f_{obs} are the calculated and observed quantities and w is a weighting factor. (The program contains a set of default weightings and we used these.) The program attempts to minimize S by varying the parameters of the potentials. The minimization uses the Newton–Raphson algorithm with numerical first derivatives. At first we only allowed a couple of parameters to vary during a fitting run and then we increased the number of parameters allowed to vary. During this stage we kept the parameters describing the dispersive term fixed since these have a reputation for not converging to physically sensible values on fitting. Once we had optimized all the parameters except those describing the dispersive terms (including the charges on the ions), we allowed the dispersive terms to vary as well.

The structures of hydroxyapatite, chloroapatite and fluoroapatite used are given in table 1. The data are taken from Hughes *et al* (1989). However, both the hydroxide ion and the chlorine ion are disordered. This is to say, they are equally likely to be found in either of two sites, above or below a symmetry position. In these simulations they have been replaced by averaged ions at symmetry positions and it is these symmetry positions that are given in table 1. The hydroxide ion is treated as a single compound ion. (Note that a monoclinic phase of hydroxyapatite in which the hydroxide ions are ordered is possible (see for example Elliot *et al* 1973). This requires pure, stoichiometric hydroxyapatite and is a laboratory curiosity which never occurs in nature.) The parameters of the potentials resulting from the fitting process are given in table 2. One unusual feature of the resulting model is that the charge on the Ca ion becomes larger than its formal charge. In table 3 the predictions of the model for the lattice parameters, elastic constants and vibrational frequencies are compared with experiment. The predicted lattice parameters and elastic constants of a fluoroapatite model recently developed by Meis *et al* (2000) are also given for comparison.

3. Relaxation processes

If a cut is made in a bulk solid, creating a surface, the configuration of the atoms close to the surface changes (Houchmandzadeh *et al* 1992). In the bulk, the forces on the atoms are perfectly balanced; however, when part of the bulk is removed to create a surface, the forces on the atoms are no longer balanced and the atoms move in response to these forces. Another way of understanding what can happen at a surface is through a consideration of symmetry. Many of the symmetries of the bulk crystal are broken at the surface: translational symmetry not parallel to the surface, mirror planes not perpendicular to the surface, rotation axes not perpendicular to the surface etc. The breaking of these symmetries will lead to the readjustment of the crystal structure—in the regions close to the surface where the broken symmetry is 'felt'—to structures consistent with the symmetry of the crystal surface. For example, at a surface the direction normal to the surface pointing outward is not equivalent to the direction normal to the surface pointing inward. Therefore the symmetry of the surface layers does not forbid the system to

Table 1. Structures of hydroxyapatite, chloroapatite and fluoroapatite taken from Hughes *et al* (1989). The x-axis is denoted by x^* because it is not orthogonal to the y-axis. A hexagonal coordinate system is used in which the x- and y-axes are at 120° to each other.

	Fluoroapatite	Hydroxyapatite	Chloroapatite
Space group	$P6_3/m$	$P6_3/m$	$P6_3/m$
Unit-cell parameters			
a (Å)	9.3973	9.4166	9.5979
c (Å)	6.8782	6.8745	6.7762
Fractional coordinates of asymmetric unit			
Ca(1)			
x^*	2/3	2/3	2/3
y	1/3	1/3	1/3
z	0.0010	0.00144	0.0027
Ca(2)			
x^*	−0.00712	−0.00657	0.00112
y	0.24227	0.24706	0.25763
z	1/4	1/4	1/4
P			
x^*	0.36895	0.36860	0.37359
y	0.39850	0.39866	0.40581
z	1/4	1/4	1/4
O(1)			
x^*	0.4849	0.4850	0.4902
y	0.3273	0.3289	0.3203
z	1/4	1/4	1/4
O(2)			
x^*	0.4667	0.4649	0.4654
y	0.5875	0.5871	0.5908
z	1/4	1/4	1/4
O(3)			
x^*	0.2575	0.2580	0.2655
y	0.3421	0.3435	0.3522
z	0.0705	0.0703	0.0684
X = F, OH, Cl			
x^*	0	0	0
y	0	0	0
z	1/4	1/4	1/4

have a dipole moment perpendicular to the surface even though such a polarization of the bulk is forbidden by symmetry. However, if a polarization parallel to the surface is forbidden in the bulk, it will also be forbidden at the surface, because the creation of the surface does not affect symmetry elements acting parallel to the surface (unless a surface phase transition occurs). Another example would be a set of n equivalent atoms arranged at the vertices of an n-sided polygon, their equivalence due to an n-fold symmetry axis. If this axis lies parallel to a surface, then the symmetry it represents will be broken by the creation of the surface. The effect of this broken symmetry on the atoms may be visualized through the polygon described by the

Table 2. Parameters of the interatomic potential model. For an explanation of the potential types, see for example the web page http://www.ch.ic.ac.uk/gale/Research/gman12.html.

Buckingham potentials			
Species	A (eV)	ρ (Å)	C (eV Å^6)
P core–O shell	983.45	0.326	
O shell–O shell	712.36	0.066	25.8
OH core–O shell	4.714×10^5	0.199	27.9
OH core–OH core	23400.1	0.125	184.3
Ca core–O shell	521.46	0.379	
OH core–Ca core	10433.9	0.242	
F core–O shell	9.451×10^6	0.163	
F core–F core	91.19	0.055	
F core–Ca core	10433.9	0.242	
Cl core–O shell	10125.4	0.103	
Cl core–Cl core	3447.3	0.135	
Cl core–Ca core	9.853×10^7	0.143	
Spring potential			
Species	k (eV Å^{-2})		
O core–O shell	89.34		
Three-body potential			
Species	k (eV rad^{-2})	θ_0 (deg)	
O shell–P core–O shell			
	1.686	109.47	
Charges			
Species	Z (e)		
Ca core	2.150		
P core	4.345		
O core	1.126		
O shell	−3.024		
OH core	−1.0		
F core	−1.0		
Cl core	−1.0		

n atoms. In the bulk crystal this polygon is, due to symmetry, completely regular. However, at the surface the symmetry that requires the polygon to be regular no longer exists. It will become compressed or dilated in a direction perpendicular to the surface.

The relaxations which occur can be placed in one of two categories. The first category of relaxations only occur very close to the surface; these relaxations have the effect of reducing the surface energy of the system. The second category of relaxations penetrate some distance from the bulk. Not only do these relaxations reduce the surface energy, but also they provide an energy of interaction between opposite surfaces, due to the overlap of the relaxations from these surfaces if the two surfaces are not to far apart, i.e. if the slab is not too thick.

A mathematical description of these symmetry-breaking processes may be effected using Landau theory, which deals with the breaking of symmetry in a second-order phase transition. However, care must be taken with this: in a second-order phase transition, a symmetry described by a single order parameter is broken. At a surface the symmetry breaking is so profound that it cannot be described by a single order parameter, so a formal description would require many order parameters. On the other hand, if a single order parameter is more

Table 3. Comparison of theory and experiment. The experimental elastic constants are for an unspecified form of apatite and assumed to be applicable to all three forms of apatite.

	Fluoroapatite			Hydroxyapatite		Chloroapatite	
	Experiment	Theory[a]	Theory[b]	Experiment	Theory[a]	Experiment	Theory[a]
Lattice parameters (Å)							
a	9.3973	9.5153	9.3688	9.4166	9.5280	9.5973	9.5806
c	6.8782	6.6457	6,8694	6.8745	6.6077	6.8782	6.5634
Elastic constants (10^{10} Pa)							
C_{11}	16.67	15.28	16.46	16.67	15.33	16.67	15.12
C_{33}	13.96	13.47	—	13.96	13.60	13.96	16.14
C_{12}	1.396	5.69	—	1.396	5.69	1.396	5.35
C_{13}	6.63	6.05	5.47	6.63	6.13	6.63	6.77
C_{55}	6.63	3.32	5.47	6.63	3.41	6.63	1.74
Phosphate modes (cm^{-1})							
ν_1	420	420	—	420	420	420	419
ν_2	567	569	—	567	568	567	565
ν_3	938	939	—	938	939	938	935
ν_4	1017	1017	—	1017	1017	1017	1018

[a] This work.
[b] Meis *et al* (2000); quantities not given by Meis are marked with a dash.

important than all the others are, then a Landau theory may be written describing just that single order parameter. In the case of the surface relaxation in apatite, the material property relaxing is the polarization and the relaxation is oscillatory, so a two-component order parameter is used.

We write

$$P(z) = A(z)\sin kz + B(z)\cos kz \tag{3.1}$$

where $A(z)$ and $B(z)$ are slowly varying functions of z (compared to the oscillatory components).

The free energy describing the relaxation can be written as

$$F[P] = \int_0^L \left[\frac{a}{2}(A^2+B^2) + \frac{a}{2K^2}\left(\left(\frac{\partial A}{\partial z}\right)^2 + \left(\frac{\partial B}{\partial z}\right)^2\right)\right] \mathrm{d}z - \alpha\left[A\sin(kL+\phi) + B\cos(kL+\phi)\right]_{z=L}. \tag{3.2}$$

There are two terms, a bulk term and a surface term. The form of the bulk term ensures that the equilibrium value of the polarization in the bulk of the crystal is zero and that the functions A and B cannot vary too quickly with z. The boundary term is a coefficient, α, multiplied by a linear combination of the polarization P and its spatial gradient at the surface. This free-energy functional only describes half the system, i.e. the total size of the system is $2L$. The form of the surface relaxation in the other half of the system is determined by symmetry. This term ensures that the polarization is nonzero at the surface and thus that a surface relaxation occurs. The resulting polarization profile is obtained by minimizing the free-energy functional equation (3.2), with respect to the functions A and B:

$$P(z) = \frac{\alpha K}{a}\left(\frac{\cosh Kz\sin(kL+\phi)\sin kz}{\sinh KL} + \frac{\sinh Kz\cos(kL+\phi)\cos kz}{\sinh KL}\right). \tag{3.3}$$

The surface relaxation modifies the form of the surface energy from a constant to

$$\sigma = \sigma_0 - \frac{\alpha^2 K}{2a}(\coth KL \sin^2(kL + \phi) + \tanh KL \cos^2(kL + \phi) - 1). \quad (3.4)$$

We considered various relaxations which could occur in hydroxyapatite close to the surface. These were polarization of the atomic layers, distortions of the phosphate ions and distortions of the channels in which the hydroxide ions sit. Our calculations were for systems with two surfaces. In addition to investigating the relaxations themselves, we also calculated the energy of interaction between the two surfaces. We used the program MARVIN (Gay and Rohl 1995) to perform the relaxations for (100) surfaces.

Looking down the *c*-axis of bulk hydroxyapatite, one can see that the structure contains channels in which the hydroxide ions sit. The edges of the channels are defined by calcium ions. As required by the hexagonal symmetry of hydroxyapatite, the channels in the bulk are hexagonal. In a system with (100) surfaces, the hexads (axes of sixfold symmetry) lie parallel to the surface: the symmetry that they represent will be broken by the presence of the surface. Therefore we expect that close to the surface the hexagonal channels will be distorted. As a quantitative measure of this distortion we take the standard deviation of the perpendicular distance from the calcium ions defining the edges of the channel to the centre of the channel (measured in Å). This is shown in figure 1. The graph shows that the distortion is only significant in the hydroxide channels immediately adjacent to the surface. In fact, although the distortion of the channels only occurs close to the surface, this does not mean that it is small. Indeed the distortion is so large that it can be seen visually. Figure 2 attempts to demonstrate this. Figure 1 shows distortions of the hydroxide channels for a slab of ten unit

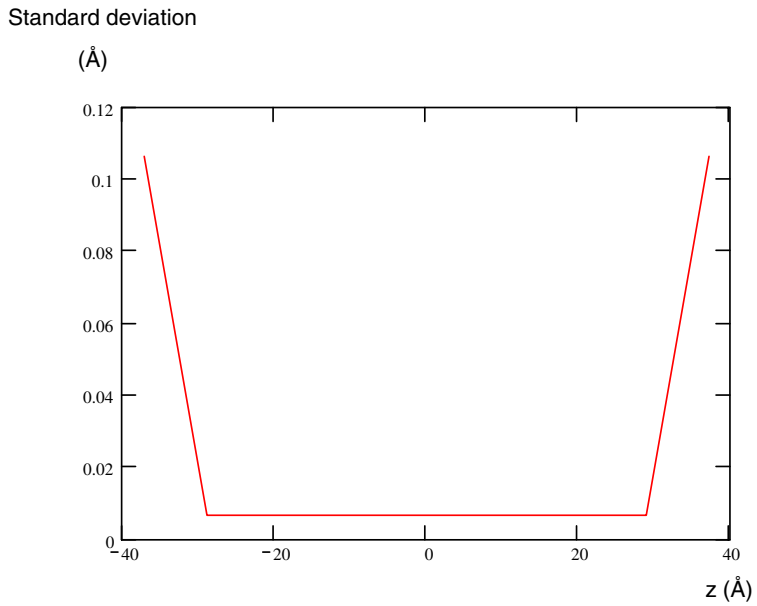

Figure 1. The distortion of the hydroxide channels in the apatite structure by the surface relaxation. The hydroxide channels are parallel to the surface and thus should be distorted by the surface relaxation since the symmetry which determines their shape in the bulk is broken by the surface. The channels are defined by the calcium ions that surround them. Therefore the standard deviation of the distances of the calcium ions surrounding the channel from the centre of the channel is used as a quantitative measure of the distortion of the channel.

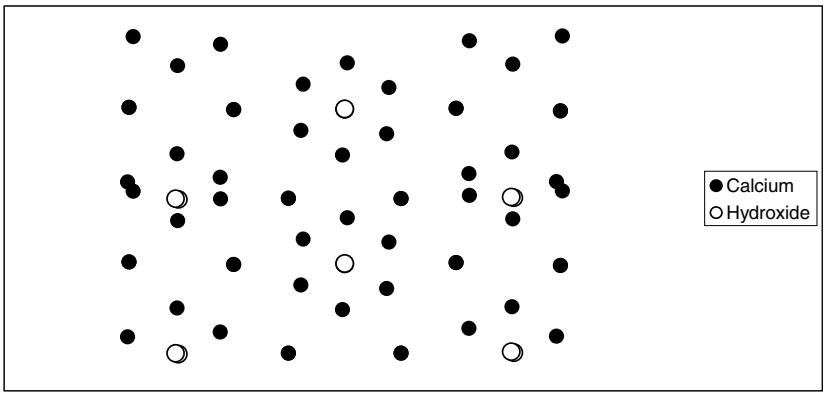

Figure 2. The view looking down the phosphate channels of a three-layer system. Crystallographically, the *c*-axis is passing into the plane of the paper and the *b*-axis is vertical. The surfaces are to the left and right of the diagram. The hydroxide ions (open circles) sit in channels formed by calcium ions (closed circles). Looking down the two central channels we can see that those channels appear to be perfectly hexagonal. However, the channels closer to the surface are clearly distorted from a hexagonal shape.

cells' thickness. In figure 2 the slab is only three layers of unit cells thick. The perspective of figure 2 is looking down the crystallographic *c*-axis, i.e. looking down the hydroxide channels. Six hydroxide channels are visible in the figure. Two of them are adjacent to the surface on the left, two of them are in the middle and two are adjacent to the surface on the right. The hydroxide channels are defined by the calcium ions surrounding them. The bulk symmetry requires that these calcium ions appear to lie on the vertices of a regular hexagon when looking down the *c*-axis. This appears to be the case for the two hydroxide channels in the centre of the system. However, the polygons formed by the calcium ions surrounding the hydroxide channels adjacent to the surfaces of the system are clearly very irregular. This shows that the distortion of the crystal structure at the surface is very large.

Another way in which surface relaxations could manifest themselves in the hydroxyapatite crystal structure is through a distortion of the tetrahedral phosphate ions. As there are no fourfold rotation–inversion axes in the symmetry group of hydroxyapatite, we do not expect the phosphate ions to have perfect tetrahedral symmetry even in the bulk. However, the surface relaxation could cause an increased degree of distortion in those phosphate ions closest to the surface. We used two quantitative measures of the distortion of the phosphate tetrahedra. The first was the standard deviation of the P–O bond length within a phosphate tetrahedron. This is shown in figure 3 for a system ten layers of unit cells thick. As can be seen, the degree of distortion measured this way only increases significantly from the bulk values for tetrahedral phosphate ions in unit cells immediately adjacent to the surface. The second quantitative measure of distortion of the phosphate ions that we used was their internal dipole moment measured in units of e Å where e is the magnitude of the electron charge (contributions to the dipole moment from core–shell separations were included). Figure 4 shows the dipole moment of the phosphate tetrahedra for a system ten layers of unit cells thick. There is no phosphate ion polarization to speak of along the x-axis, which is as it should be since the x-axis is parallel to the crystallographic b-axis. The b-axis is related by symmetry to the $-b$-axis; therefore dipole moments along this direction are forbidden by symmetry in the bulk and this symmetry is not broken by the surface. There are however nonzero phosphate-ion polarizations along the y- and z-axes. The y-axis is parallel to the crystallographic c-axis and the z-axis is normal

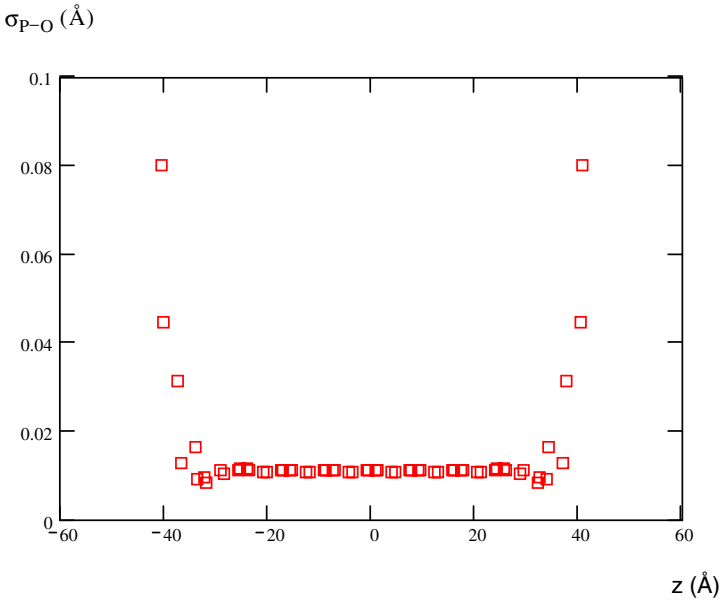

Figure 3. This shows the distortion of phosphate ions as a function of phosphate-ion coordinate for a system ten unit cells thick. The distortion is measured by the standard deviation of the P–O bond lengths measured in ångströms. Clearly, the distortion is significant only close to the surface.

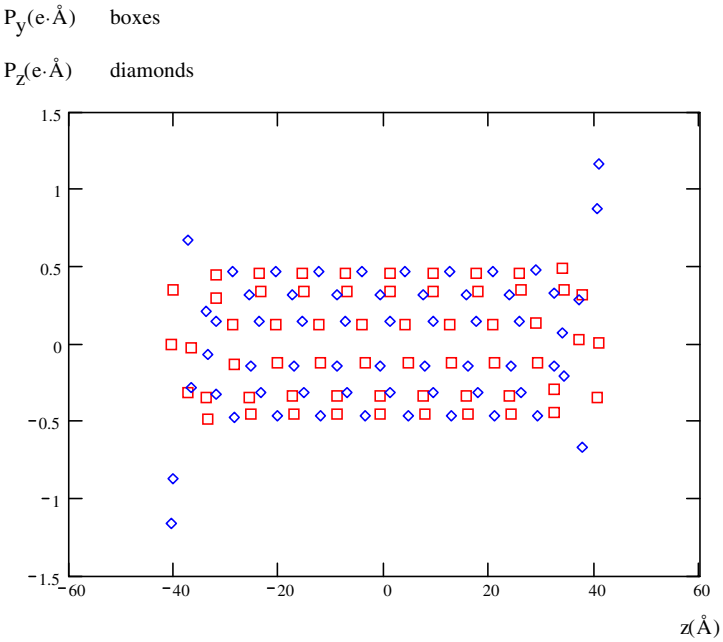

Figure 4. Distortion of phosphate ions as measured by their internal dipole moment in a system ten unit cells thick. The x-axis dipole is too small to be worth including on this graph. Only the z-axis dipole moment departs substantially from its bulk range of values and that is only for phosphate ions closest to the surface. To calculate the dipole moment, charges were taken in units of e and distances taken in units of Å.

to the (100) plane. Only the polarization parallel to the z-axis departs for the bulk range of values and then only very close indeed to the surface.

The last relaxation process that we considered was the polarization of the layers of unit cells perpendicular to the surface. Although all of the other relaxations that we considered were restricted to the surface layer, the relaxation of the polarization persists for a few unit cells' distance into the bulk. This polarization is shown in figure 5 (again contributions to this polarization from core–shell separations are included). As can be seen, the polarization relaxation is oscillatory. Since we have a relaxation that extends for some distance into the bulk of the material, we expect there to be an associated surface interaction energy. This is indeed the case as can be seen from figure 6, which shows the surface energy of a (100) surface as a function of its distance from an opposite (100) surface. The surface interaction energy is the part of the surface energy which is not constant. As one would expect, the surface energy oscillates with the separation between surfaces. This makes sense because the surface interaction energy depends on the degree of overlap between the surface relaxations from the opposite surfaces and since the relaxation is oscillatory the degree of overlap will oscillate as well.

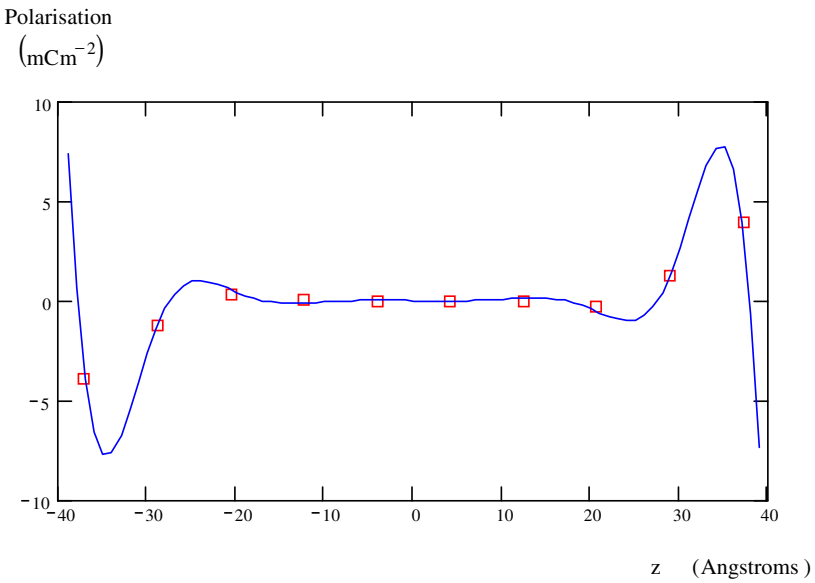

Figure 5. The polarization of hydroxyapatite layers in a system ten layers thick. This shows an oscillatory relaxation that clearly persists beyond the layer closest to the surface. The polarization is measured in mC m^{-2}; the coordinate perpendicular to the surface is measured in units of Å. The line shows a fit of the form discussed in the text; the points show data obtained from MARVIN.

To show that the polarization and the surface interaction energy were indeed connected, we fitted the polarization data for the ten-layer system and surface energy data to a surface relaxation free energy of the type described above (equations (3.1)–(3.4)). Figures 4 and 5 show that the fit is quite successful. The parameters of the fit are given in table 4. One thing which is worth commenting on is the form of the fit of the polarization. The fit shown is certainly not the simplest fit of the polarization data to the form given in equation (2.1), but the form of the fit shown is conditioned by the requirement that the same parameters K and k (see table 4) describe both the polarization and the surface interaction energy.

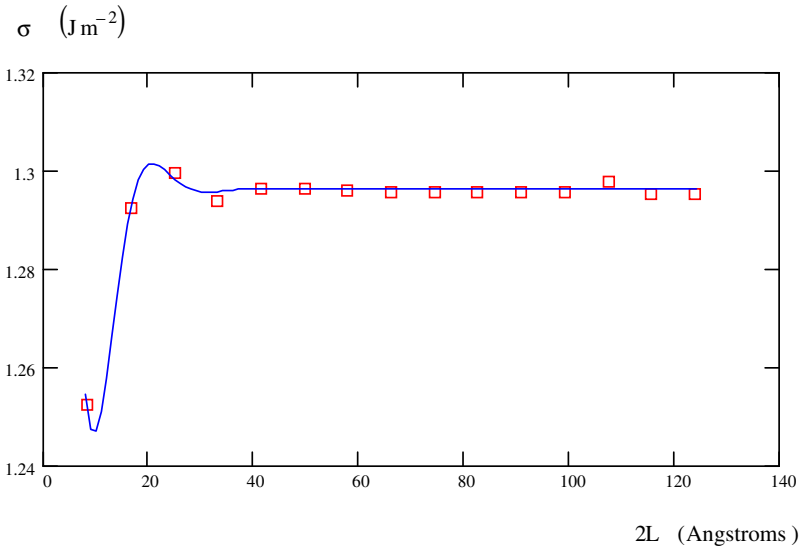

Figure 6. Surface energy as a function of thickness. Because the relaxation oscillates, the surface energy oscillates as well. The surface energy is measured in J m^{-2}. L is half the distance separating the surfaces. The line shows a fit of the form discussed in the text; the points show data obtained from MARVIN.

Table 4. Parameters used to fit the polarization and the surface energy of the apatite (100) surfaces.

Parameter	Value
σ_0	1.296 J m^{-2}
$\alpha^2 K/2a$	0.183 J m^{-2}
$\alpha K/2a$	−34.5 mC m^{-2}
ϕ	2.88 rad
K	0.196 Å^{-1}
k	0.301 Å^{-1}

4. Implications for the growth morphology of bone apatite

One of the unsolved problems of the growth of bones in humans and other mammals is the shape of the crystals grown in them. The mineral portion of bone is a carbonate-substituted hydroxyapatite. When hydroxyapatite is grown from solution it grows with a needle morphology, long dimension 20 nm, diameter 5 nm (Posner *et al* 1984). However, the apatite crystals in bones are platelet shaped. Furthermore, because the crystals are so small, their morphology should mimic the crystal symmetry, i.e. have hexagonal symmetry. The bone apatite crystals have the hexagonal axis lying in the plane of the platelet (Landis *et al* 1996)

One possible explanation for this morphology is the symmetry-breaking platelet growth mechanism proposed by Lee *et al* (1999). This mechanism relies on a surface relaxation large enough to make the surface energy negative at small surface separations. Our results do not show that this is the case for apatite and indeed we would not expect them to, because the platelet growth morphology does not occur when hydroxyapatite is precipitated *in vitro*. However, we speculate that it may be possible that in the *in vivo* growth of apatite the body may manipulate the growth conditions so as to allow the platelet growth mechanism to work.

Both the carbonate impurities in apatite and the various organic molecules found in bones may be involved in altering both the surface energy and the surface relaxation of apatite. The carbonate impurity concentration may well couple to the order parameter of the surface relaxation, so if impurities were more stable at the surface, then the coupling would alter the boundary conditions of the surface relaxation, making the magnitude of the relaxation larger and thus increasing the surface interaction energy. The organic molecules found in bones may have several effects if they adhere to the apatite surface. Firstly, they can influence the surface relaxation directly by altering the boundary conditions at the surface. They can also affect it indirectly by attracting impurities to the surface. Lastly, and most importantly, they can also influence the surface energy, reducing it to a value which allows the platelet growth mechanism to work. At the time of writing, all the above is speculative and it will be necessary to prove that the effects described above exist and that their magnitude is large enough to account for the platelet morphology of bone apatite.

Appendix

In this appendix we consider the extent to which we expect that an interatomic potential model designed to reproduce bulk properties will be successful in predicting the surface relaxation and the surface interaction energy. An interatomic potential model can be described by a potential energy function of atomic displacements. This potential energy term can be expanded as a power series in the atomic displacements. The quadratic terms determine the elastic constants and the phonon frequencies, so we expect that it will be possible to determine these quadratic terms with a reasonable degree of accuracy by fitting to elastic and vibrational data. In terms of describing the surface relaxation, the quadratic terms determine the parameters a, K and k of equations (3.1)–(3.4). The linear terms in the expansion however cannot be determined by fitting to bulk properties. The only constraint which the bulk properties provide is that the sum of the linear terms should be zero. This makes it unlikely that fitting to the bulk properties will select the correct individual linear terms. When there is a surface, on the other hand, the linear terms no longer sum to zero because some of the atoms are missing. In this case the individual terms become important. In terms of the surface relaxation, the linear terms determine the parameters α and ϕ of equations (3.1)–(3.4). α and ϕ in turn determine the magnitude of the surface relaxation (proportional to α; see equation (3.3)) and the magnitude of the energy of interaction between surfaces (proportional to α^2; see equation (3.4)).

To show this in more detail, we consider a pair potential potential energy:

$$V = \sum_{ij} f_{ij}(u_i - u_j) \tag{A.1}$$

where f_{ij} is the potential energy between atoms i and j. It is a function of the relative displacements of atoms i and j. The individual vector displacements of atoms i and j are u_i and u_j respectively. The sum is over all pairs of atoms.

We expand this potential energy to quadratic order in the displacements:

$$\begin{aligned} V &= \sum_{ij} f_{ij}(0) + \sum_{ij} (u_i - u_j)\frac{\mathrm{d}f_{ij}}{\mathrm{d}u}\bigg|_{u=0} + \frac{1}{2}\sum_{ij}(u_i - u_j)^2\frac{\mathrm{d}^2 f_{ij}}{\mathrm{d}u^2}\bigg|_{u=0} \\ V &= \sum_{ij} f_{ij}(0) + \sum_i u_i \sum_j \left(\frac{\mathrm{d}f_{ij}}{\mathrm{d}u}\bigg|_{u=0} - \frac{\mathrm{d}f_{ji}}{\mathrm{d}u}\bigg|_{u=0}\right) \\ &\quad + \frac{1}{2}\sum_i u_i^2 \sum_j \left(\frac{\mathrm{d}^2 f_{ij}}{\mathrm{d}u^2}\bigg|_{u=0} + \frac{\mathrm{d}^2 f_{ji}}{\mathrm{d}u^2}\bigg|_{u=0}\right) - \sum_{ij} u_i u_j \frac{\mathrm{d}^2 f_{ij}}{\mathrm{d}u^2}\bigg|_{u=0}. \end{aligned} \tag{A.2}$$

The first term is simply the bulk free energy. The third and fourth terms determine the elastic constants and the phonon frequencies of the material: see for example Landau and Lifshitz (1980). Therefore we expect that it will be possible to determine these terms accurately by choosing potentials to reproduce bulk properties. However, the only constraint that can be put on the second term is that the sum over j must come to zero. There is no way that the individual terms of the sum over j can be determined by considering bulk properties. In the case of calculating bulk properties, a knowledge of the values of the individual terms is unnecessary; however, for calculating surface relaxations it is essential. When there is a surface, some of the terms in the sum over j will not be present because the atoms to which they refer are absent. Thus in the case of a surface, the sum over j will no longer be zero and its value (and sign) will depend on the size of the individual terms. Therefore we cannot in general expect an interatomic potential model chosen to reproduce bulk properties to accurately predict the magnitude or even the sign of the surface relaxation. This problem can be overcome in two ways. Firstly, if some information about the surface relaxation is known, then this could be used to improve the potentials. Secondly, nonempirical methods, e.g. *ab initio* electronic structure calculations, could be used.

References

Bhimasenachar J 1945 Elastic constants of apatite *Proc. Indian Acad. Sci.* **22** 209–14

Bush T S, Gale J D, Catlow C R A and Battle P D 1994 Self-consistent interatomic potentials for the simulation of binary and ternary oxides *J. Mater. Chem.* **4** 831–7

Elliot J C, Mackie P E and Young R A 1973 Monoclinic hydroxyapatite *Science* **180** 1055–7

Farmer V C 1974 *Infrared Spectroscopy of Minerals* (London: Mineralogical Society)

Gale J D 1997 GULP: a computer program for the symmetry-adapted simulation of solids *J. Chem. Soc. Faraday Trans.* **93** 629–37

Gay D H and Rohl A L 1995 MARVIN: a new computer code for studying surfaces and interfaces and its application to calculating the crystal morphologies of corundum and zircon *J. Chem. Soc. Faraday Trans.* **91** 925–36

Houchmandzadeh B, Lajerowicz and Salje E 1992 Relaxations near surfaces and interfaces for first-, second-, and third-neighbour interactions: theory and applications to polytypism *J. Phys.: Condens. Matter* **4** 9779–94

Hughes J M, Cameron M and Crowley K D 1989 Structural variations in natural F, OH and Cl apatites *Am. Mineral.* **74** 870–6

Landau L D and Lifshitz E M 1980 *Statistical Physics* Part 1 (Oxford: Butterworth–Heinemann)

Landis W J, Hodgens K J, Arena J, Song M J and McEwen B F 1996 Structural relations between collagen and mineral in bone as determined by high voltage electron microscopic tomography *Microsc. Res. Tech.* **33** 192–202

Lee W T, Salje E K H and Dove M T 1999 Effect of surface relaxations on the equilibrium growth morphology of crystals: platelet formation *J. Phys.: Condens. Matter* **11** 7385–410

Meis C, Gale J D, Boyer L, Carpena J and Gosset D 2000 Theoretical study of Pu and Cs incorporation in a mono-silicate neodymium fluoroapatite $Ca_9Nd(SiO_4)(PO_4)_5F_2$ *J. Phys. Chem.* A **104** 5380–7

Parker S C and Baram P S 1996 Atomistic simulation of hydroxide ions in inorganic solids 1996 *Phil. Mag.* B **73** 49–58

Posner A S, Blumenthal N C, and Betts F 1984 Chemistry and structure of precipitated hydroxyapatites *Phosphate Minerals* ed J O Nriagu and P B Moore (New York: Springer)

Sanders M J, Leslie M and Catlow C R A 1984 Interatomic potentials for SiO_2 *J. Chem. Soc. Chem. Commun.* 1271–3

Weiner S and Wagner H D 1998 The material bone: structure-mechanical function relations *Annu. Rev. Mater. Sci.* **28** 271–98